



Inundation time mediates denitrification end products and carbon limitation in constructed floodplains of an agricultural stream

Martha M. Dee · Jennifer L. Tank

Received: 14 October 2019 / Accepted: 26 April 2020 / Published online: 8 May 2020
© Springer Nature Switzerland AG 2020

Abstract Conversion of landscapes to large-scale agriculture has substantially increased the loading of bioavailable nitrogen (N) to stream networks through extensive artificial drainage and fertilizer application. Floodplain restoration may enhance N cycling in agricultural stream systems by increasing residence time of floodwaters in contact with bioreactive surfaces that retain or remove excess N. Microbially-mediated denitrification potentially plays a significant role in constructed floodplains by permanently removing excess N through conversion of bioavailable nitrate ($\text{NO}_3\text{-N}$) to dinitrogen gas, either as N_2O or N_2 . Restoring channelized streams via the construction of inset floodplains can increase the total denitrification capacity of agricultural watersheds, but little is known about the abiotic factors that control the proportion of $\text{NO}_3\text{-N}$ that is converted to the potent greenhouse gas N_2O versus N_2 (i.e., N_2O yield). We used an in-situ static core design to assess the

importance of constructed floodplain age, inundation time, and carbon (C) availability on total denitrification rates and N_2O yield. Novel use of membrane-inlet mass spectrometry (MIMS) allowed us to simultaneously measure N_2O and N_2 to capture total denitrification and the proportion of bioavailable N converted to each end-product. Floodplain age did not influence total denitrification rates, but rather denitrification increased with the duration of floodplain inundation until C limitation occurred at approximately 24 h. In addition, we found that N_2O yields from floodplain soils were higher than those reported for other aquatic systems. Finally, while floodplain restoration in agricultural streams generally increases N retention at the watershed scale, regardless of the restoration age, the impact of added floodplains on N_2O emissions should be considered.

Keywords Agricultural streams · Denitrification · Floodplains · Greenhouse gas · Membrane-inlet mass spectrometry · Nitrous oxide (N_2O) · Two-stage ditch

Responsible Editor: James Sickman.

M. M. Dee (✉)
Michigan Sea Grant, Michigan State University
Extension, 184 US-41 E, Negaunee, MI 49866, USA
e-mail: gerigmar@msu.edu

J. L. Tank
Department of Biological Sciences, University of Notre
Dame, 189 Galvin Life Sciences, Notre Dame,
IN 46556, USA
e-mail: tank.1@nd.edu

Introduction

In the agricultural Midwestern US, extensive fertilizer application and artificial drainage have resulted in high nitrogen (N) loading rates to adjacent waterways (Vitousek et al. 1997), which can contribute to

decreased water quality in downstream receiving waters (Carpenter et al. 1998). Stream channelization and subsurface tile drainage allow for the efficient removal of excess water from low-gradient agricultural lands (Landwehr and Rhoads 2003), but these practices reduce streamwater contact time with stream sediments and floodplain soils that may promote biological N removal (Randall et al. 1997; Bukavekas 2007). Moreover, in many agricultural streams, nitrate ($\text{NO}_3\text{-N}$) uptake is typically saturated due to very high loading from the surrounding landscape (Bernot et al. 2006). Therefore, optimizing N removal is a priority for restoration strategies in agricultural streams (Groffman and Crawford 2003; Sheibley et al. 2006; Kaushal et al. 2008; Roley et al. 2012a, b). A shared goal among farmers and resource managers is to maintain agricultural productivity while minimizing negative environmental impacts. We investigate how one approach (i.e., floodplain restoration) contributes to that goal.

A common goal for agricultural conservation practices is to optimize biological N removal while still maintaining the drainage needs of the adjacent agricultural land (Roley et al. 2012a). While many streams in the agricultural Midwest have been channelized to improve drainage from the landscape, the resulting channel often suffers from bank slumping, undercutting and sediment deposition (Landwehr and Rhoads 2003). Therefore, to increase N retention and channel stability while accommodating the needs of surrounding farmland, land managers have implemented an alternative strategy whereby inset floodplains are constructed alongside the stream channel, called two-stage floodplains (Powell et al. 2007), which allow tile drain water to flow directly onto floodplains during baseflow conditions, and during storms, slows down floodwaters which inundate adjacent floodplains (Roley et al. 2012a). Previous studies have shown that the increased residence time on these constructed floodplains, whose design mimics that of natural floodplains, enhances denitrification (Roley et al. 2012a, b; Mahl et al. 2015; Hanrahan et al. 2018), which is a microbially-mediated process by which $\text{NO}_3\text{-N}$ is converted to dinitrogen gases under anoxic conditions and in the presence of organic carbon (C; Knowles 1982). While studies have compared denitrification in two-stage versus channelized ditches (Powell and Bouchard 2010; Roley et al. 2012a) as well as unmaintained, “naturalized” ditches

(Hanrahan et al. 2018), few studies have compared denitrification in constructed floodplains of different ages.

Although denitrification results in a permanent removal of dissolved N from the system as the inert gaseous compound of N_2 (Galloway et al. 2003), it can also produce N_2O in its incomplete form. The production of N_2O as an intermediate form occurs when nitrous oxide reductase activity (*nos*), the enzyme that reduces N_2O to N_2 , is suppressed and denitrifying bacteria cannot complete the full reduction pathway (Firestone et al. 1979). The suppression of this enzyme has been found by previous studies to occur under high soil $\text{NO}_3\text{-N}$ concentrations (Jalota et al. 2018; Weier et al. 1991), among other abiotic factors including temperature, pH, and soil moisture (Smith et al. 2003). The fraction of denitrified N that escapes the system as N_2O versus N_2 (i.e., N_2O yield) is an important metric, but our understanding of factors that control this ratio in stream floodplains is limited (Beaulieu et al. 2011).

Nitrous oxide is a potent greenhouse gas, with ~ 300 times the warming potential than that of carbon dioxide (IPCC 2007), and anthropogenic N loading to river networks may be an important source of N_2O to the atmosphere (Beaulieu et al. 2011). Moreover, N_2O yield is an important metric that has supported global regulatory efforts (Nevison 2001), and as such, previous research has sought to understand what drives the relative proportion of denitrification end-products (Firestone et al. 1979; Letey et al. 1980; Vinther 1984; Weier et al. 1993; Beaulieu et al. 2011; Phillips et al. 2015). For example, N_2O yield (calculated as $\text{N}_2\text{O}/\text{N}_2$) decreased with incubation time and was lowest under conditions of high soil water content and C availability, while high $\text{NO}_3\text{-N}$ increased N_2O yields (Weier et al. 1993). Constraining estimates of N_2O yield for aquatic systems receiving excess N from agriculture (i.e., “indirect emissions”; Nevison 2001; Klein et al. 2006) motivated early studies (Ryden et al. 1979), but these estimates have proven to be variable and analytically challenging.

Field measurements of N_2 and N_2O produced in floodplain soils are challenging (Phillips et al. 2015), mostly because estimating N_2 is complicated by high atmospheric concentrations of the gas. Most denitrification studies have been performed using techniques that block the reduction of N_2O to N_2 , allowing for the accumulation of N_2O , which is easily measured via

gas chromatography. Others have quantified denitrification using flow-through cores that allow for the accumulation and analysis of N_2 and N_2O simultaneously (Burgin et al. 2010; Burgin and Groffman 2012). The development of membrane-inlet mass spectrometry (MIMS) has allowed for rapid, high-precision measurements of dissolved N_2 , O_2 , and Ar in water (Kana et al. 1994), and does not require headspace equilibrations (as for gas chromatography) or large sample volumes, which facilitates in-situ field experiments. In recent studies, standard MIMS methodologies have been modified to measure the presence of other dissolved gasses, including CO_2 (Gueguen and Tortell 2008), methane (CH_4 ; Schlüter and Gentz, 2008), and nitric oxide (NO; Conrath et al. 2004; Goodwin et al. 2018). However, we are aware of only a single study that has explored the capacity of MIMS to accurately measure N_2O and N_2 simultaneously (Genthner et al. 2013), who used an ultralow freezer as a cryotrap for the measurement of N_2O .

In this study, we compared total denitrification rates (measuring both $N_2 + N_2O$ accumulation) in constructed floodplain soils (via the two-stage ditch) constructed in 2007 and 2017, and examined the environmental factors that potentially control N_2O yields in floodplain soils. Specifically, we tested the role of inundation and C availability using in situ cores containing overlying “floodwater” of ambient and elevated dissolved C concentrations. We hypothesized that denitrification would be higher on older floodplains, regardless of C amendment, because the combination of stream sediment deposition during flooding combined with the seasonal growth and decomposition cycles of floodplain grasses would promote C accrual. We also predicted that the end-product of denitrification would shift from N_2O to N_2 as a function of increased inundation time and C availability.

Methods

Study site

We conducted this study in the Shatto Ditch, a 9.4 km tributary of the Tippecanoe R. located in north-central Indiana, USA (Fig. 1a, c). The Shatto Ditch drains a watershed of primarily tile-drained, row crop agriculture in maize-soybean rotation, and is a system that has

historically been maintained, through periodic dredging, as a drainage ditch, resulting in incised banks with steep slopes (Fig. 1c). As a result, the system has the flashy discharge regime typical of first-order Midwestern agricultural streams (Roley et al. 2012b, 2014); its baseflow discharge ranges from 12 to 174 L/s, but flows can be up to 1000 L/s during storms (Roley et al. 2012a). Large amounts of fine benthic organic matter (FBOM) and sand are transported during high-discharge events, as the streambed is composed mainly of a homogenous mix of sand, FBOM, and small gravel typical of the outwash plain in which Shatto Ditch is located. Given the adjacent agricultural land use, > 11 years of data collection shows elevated inorganic nutrient concentrations with NO_3^- -N generally > 5 mg L⁻¹ on average (Griffiths et al. 2013; Roley et al. 2014; Hanrahan et al. 2018).

In November 2007, lateral inset floodplains were constructed along a 600 m reach of Shatto Ditch via the construction of a two-stage ditch (Roley et al. 2012a, b, 2014; Fig. 1a). Channel slopes on each side of the stream were excavated to create ~ 3 m wide inset floodplains that were allowed to vegetate naturally (Reed canary grass; *Phalaris arundinacea*), and floodplains inundate regularly (~ 12 times per year) during high flow events. In August 2017, an additional 3700 m of two-stage ditch was constructed directly upstream of the first two-stage segment (Fig. 1b) to make a total of 4.3 km of continuous two-stage ditch, the longest such construction in the world. We utilized the two different constructed floodplain reaches to compare the influence of inundation time and C amendment on denitrification rates between constructed floodplains of different ages.

Denitrification incubations using in situ, intact cores: experimental field-based design

In June 2018, we conducted in situ denitrification incubations during baseflow conditions when floodplain soils were recently wetted during a storm, but not saturated or flooded. We randomly selected a plot approximately 1 m away from the stream, on the floodplain bench, within each of the two study reaches (EST, NEW) to perform the chamber incubations. After manually clearing away the overlying vegetation to expose the floodplain soils, we deployed 0.25 m long clear acrylic cores at 5–10 cm depth to capture

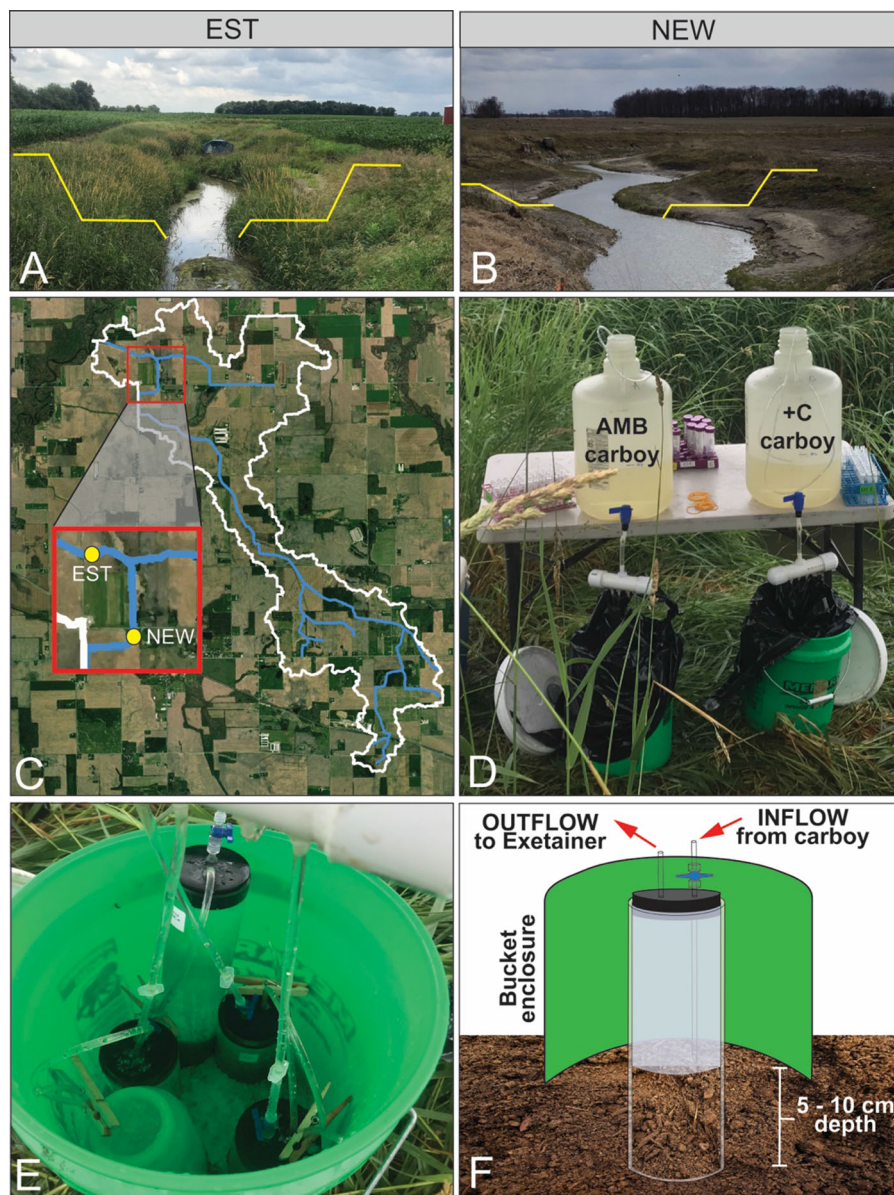


Fig. 1 Diagrams of **a** established (EST) and **b** newly constructed (NEW) two-stage ditch within the **c** Shatto Ditch watershed. Each study site was equipped with a sampling station (**d**) containing a carboy for each amendment flowing passively

the zone shown previously to have the highest denitrification activity (Roley et al. 2012a; Fig. 1e).

To inundate the chambers, we carefully collected 10L of site water from the center of the stream, with minimal artificial aeration, in two identical carboys (Fig. 1d). The first carboy provided unamended, ambient (AMB) site water and the second carboy

into a contained area with the in-situ cores (**e**). Cores are installed at 5–10 cm depth (**D**) and remain in-situ for the duration of the experiment. **f** Cross-sectional diagram of in-situ experimental setup

was amended with dextrose to elevate carbon levels (+ C) in site water by 10–15 mg L⁻¹ above ambient conditions. Tables provided an elevated surface to fill cores from carboys passively using a network of airtight tubing fitted with stopcocks to regulate flow (Fig. 1d). We deployed 3 soil cores per treatment (AMB, + C) protected from the elements by a

bottomless 5-gallon bucket at each site (EST, NEW), and included a single control core filled with treatment water only in each bucket ($n = 4$; Fig. 1e). We sealed the cores with rubber stoppers (size 13) fitted with an inlet tube regulated with a stopcock and an outlet tube fitted with a stopcock used for sampling (Fig. 1f). The inlet tubes for each core within each treatment ($n = 4$) were directly connected to a T-junction at the spigot of the carboy and therefore allowed for direct, gravity-fed regulation of water flow to the cores at the time of sampling. These deployed cores remained intact and stationary for the entire duration of the experiment, approximately 56 h.

To characterize stream conditions at the time of sampling, we collected and filtered three replicate water samples (60 mL) adjacent to each core deployment site and kept them frozen until analysis for NO_3^- -N using the cadmium reduction method (APHA 2012). We took 3 replicate floodplain soil cores with a push corer (5-cm depth X 2.2. cm diameter; Model HA, Oakfield Apparatus, Inc., WI, USA) to characterize soil extractable nutrients. We stored samples in a sealed container at 4C, until extraction (within 3 days of collection) by adding 40 mL of 2 mol L^{-1} potassium chloride (KCl) to 4 g of soil at field moisture. We agitated samples at 100 rpm for 1 h, filtered, and the supernatant was frozen until later analysis. Extractable nutrients were expressed per unit dry mass. We analyzed surface water and soil extractions on a Lachat QC8500 Flow Injection Autoanalyzer (Lachat Instruments, Loveland, Colorado, USA).

In-situ sampling over incubation time

After we deployed the floodplain cores, and set up the gravity-feed system, we filled all cores simultaneously with water from their respective treatment carboy, and sealed them by pressing the rubber stopper securely into the top of the acrylic core, pushing any excess water and air through the outlet tube until no bubbles present within the core. Once both the inlet and outlet tubes were closed, we began the incubation period. We allowed the cores to incubate for 1 h before taking the first dissolved gas sample to allow the system to come to equilibrium (Groffman et al. 1999). At 1 h post-sealing, we opened the spigot to the carboy and opened the stopcock to the respective core, to allow water from the carboy to passively be delivered at the water–

sediment surface, displacing water at the top of the core, pushing it through the outlet tube, and filling three replicate 12 mL Exetainer vials (Labco Ltd. Lampeter, UK). We overfilled each vial three times from the bottom to minimize the sample interaction with the atmosphere and collected the overflow volume in a container to later account for dilution within the core. We added 0.2 mL of 50% w/v ZnCl_2 solution to each vial for preservation, and 0.2 mL of saturated sodium hydroxide (NaOH) solution to convert all CO_2 within the sample to bicarbonate, as the presence of CO_2 within the sample interferes with the quantification of N_2O by MIMS (Genthner et al. 2013). We sealed these vials with double-wadded Teflon Exetainer caps and stored submerged upside-down until analysis for dissolved gas concentration. We recognize the potential of disproportionate accumulation of gases in the water column above the sediments, which previous studies have controlled for by actively mixing the water column within the cores (Gihring et al. 2010) or designing a fully flow-through system (Kana et al. 1998). However, given the constraints of a fully in situ field design with high replication, we chose to proceed without physical mixing. We believe that by filling cores at each time period from the sediment–water interface allowed for periodic mixing of the water column.

We repeated this process for each treatment (AMB, + C) at each site (EST, NEW) at four sampling times, approximately 2 h apart, to total ~ 8 h incubation period (+ 1 h equilibration) for each inundation time. In addition to samples taken from the cores, we took replicate dissolved gas samples via siphon from the treatment carboys to account for dilution within the cores at each time point. Prior to leaving the site at the end of the incubation, we flushed each core with fresh water from the treatment carboys and loosely covered them with their respective stoppers. We repeated this process at 24 h post-deployment, and again at 48 h without disturbing the cores to examine how variation in the duration of floodplain inundation influences denitrification (3 inundation times: 0HR, 24HR, 48HR). After the incubation was complete for the 48HR inundation time, we removed the intact cores, transported them back to the lab, and stored them at 4C until further soil analysis.

Dissolved gas analysis by MIMS

We simultaneously analyzed dissolved di-nitrogen gas (N_2) and nitrous oxide (N_2O) using membrane inlet mass spectrometry (MIMS; Bay Instruments, Easton, MD, USA) (Kana et al. 1994, 1998). Briefly, samples are drawn from the Exetainer vial by peristaltic pump and dissolved gases are diffused over a membrane under a vacuum before being analyzed by mass spectrometry, which directly quantifies the concentration of $^{28}N_2$, $^{32}O_2$ and $^{28}N_2:Ar$, $^{32}O_2:Ar$ in the water sample. Similar to Genthner et al. (2013), we modified a typical MIMS protocol to simultaneously measure the concentration of N_2 and N_2O in our samples by utilizing a cryotrap (typically used to extract water vapor and other compounds prior to dissolved gases reaching the mass spec) held between -85 and -90 °C (Genthner et al. 2013). This range is below the freezing point of CO_2 (-78 °C), but above the freezing point for N_2O (-91 °C), which allowed the mass spec to interpret any gas with the molecular mass of 44 as N_2O instead of the equivalent CO_2 , which gave us the ability to simultaneously measure the concentration of $^{44}N_2O$ and $^{28}N_2$ in each sample. We created this cryotrap using a cost-effective mixture of dry ice and isopropanol in the absence of a portable ultralow freezer. This cryotrap contained approximately a 50:50 mixture of dry ice and isopropanol by volume in a cryogenic storage dewar, monitored constantly by an ultralow thermometer probe (VWR International, Radnor, PA, USA) inserted into the mixture. Every five samples, we ran an air-equilibrated standard consisting of a dilute NaOH solution (6.25 mL saturated NaOH solution in 1L of nanopure water at 18 M Ω resistance) held at the temperature of sample collection ($19 - 23$ °C) using a water bath (VWR International, Radnor, PA, USA) and stirring at constant speed (Lab Egg RW11 Basic, IKA Works Inc., Wilmington, NC, USA). These standards were used to correct for instrument drift throughout the course of a daily run. If core temperature differed significantly (> 2 °C) over the course of an incubation, we ran samples in separate batches with air-equilibrated standards reflecting the given temperature.

We calculated the concentration of dissolved N_2 and N_2O in each sample by multiplying the N_2 and N_2O to Ar ratios from the MIMS by the equilibrium concentration of Ar using equations based on

temperature of the water and barometric pressure of the laboratory at the time of analysis (Hamme and Emerson 2004) and corrected for field conditions. We used Ar ratios to calculate concentrations, as the MIMS is more precise with ratios than absolute concentrations. Once we calculated initial sample N_2 and N_2O concentrations in $\mu\text{mol L}^{-1}$, we multiplied each value by its respective molar mass ($N_2 = 28 \text{ g mol}^{-1}$, $N_2O = 44 \text{ g mol}^{-1}$) to acquire concentrations in $\mu\text{g L}^{-1}$. Once compiled by inundation time, site, and amendment, each set of 3 replicate dissolved gas samples were corrected by the potential dilution by the carboy water addition at the previous time point.

We used simple linear regression to determine whether there was a significant change in N_2 and N_2O concentrations (in mg L^{-1}) over incubation time for all replicates at each time point, assuming a positive linear relationship in N_2 indicates detectable complete denitrification (CDN; Groffman et al. 1999) and an increase in N_2O indicates detectable incomplete denitrification (IDN). The slope of the line equals the rate of the process (as $\mu\text{g N}_2$ (or N_2O) $\text{L}^{-1} \text{ h}^{-1}$). We multiplied these rates by the volume of overlying water present within each respective core, measured in the field (distance in cm from water–sediment surface to bottom of the rubber stopper \times horizontal surface area of core), expressed in $\mu\text{g h}^{-1}$. We assume that these measurements are representative of the entire water column within the core due to the mixing that occurred as a result of adding water near the sediment–water interface. If regressions were statistically insignificant, we considered denitrification to be below our detection limits. To place CDN and IDN in the same units, we expressed rates of N_2 and N_2O production as $N_2\text{-N}$ and $N_2O\text{-N}$, respectively, as well as adding them together to express total denitrification (TDN; in $\mu\text{g N h}^{-1}$), reflecting the sum of the rates of $N_2\text{-N}$ and $N_2O\text{-N}$ denitrification. In the cases when denitrification was significant for only one of the N gas species, we calculated TDN as simply the rate of the significant species. To compare with previous studies, we expressed rates of TDN in three different ways: (1) as areal fluxes by dividing by the core surface area (0.0032 m^2 ; $\mu\text{g N m}^{-2} \text{ h}^{-1}$), (2) per g of sediment ash-free dry mass (AFDM; $\mu\text{g N [g AFDM]}^{-1} \text{ h}^{-1}$, denoted as DN_{AFDM}), and (3) per g of sediment dry mass (DM; $\mu\text{g N [g DM]}^{-1} \text{ h}^{-1}$, denoted as DN_{DM}).

Laboratory analysis of floodplain soil characteristics

Once all inundation times were complete, we analyzed the stored soil cores for a suite of biophysical characteristics to examine controls on denitrification between the two sites (EST, NEW). We transferred the soil from each core into separate, pre-weighed aluminum tins. We dried the entirety of the core at 60 °C until the weight was consistent (~ 90 h) to calculate DM. We crushed and homogenized any large pieces of soil to ensure even and thorough ashing in the muffle furnace at 550 °C for 4 h to calculate AFDM. We estimated percent organic matter (OM) for each soil core using the ratio of AFDM to DM (Arango et al. 2007). Prior to ashing the cores, we also took three replicate subsamples from each core to determine total carbon (C) and nitrogen (N) content. We weighed ~ 20 mg of ground soil into 5 × 9 mm tin capsules (Costech, Valencia, CA) and measured total C, total N, and C:N ratio of each core on an elemental analyzer (Costech ECS 4010, Valencia, CA).

Upscaling denitrification along the stream reach

After measuring denitrification rates in cores, we scaled our results to the constructed floodplain area of Shatto Ditch, to determine total N removal via denitrification, multiplying the area of floodplain (in m²) by the areal denitrification rate (μg N m⁻² h⁻¹) for a given inundation. We scaled denitrification for two different periods of floodplain restoration: (1) post-2007 and (2) post-2017. Post-2007 refers to the period of 2007–2017 during which the initial 600 m reach was constructed (1800 m²). Post-2017 refers to the restoration of a 3700 m (11,104 m²) reach performed in August 2017 and period in which the remaining available stream reach was constructed in 2018 (8208 m²). In order to estimate reach-scale N-removal potential of Shatto Ditch, we applied a recently-published denitrification rate for naturalized floodplains (726 μg N m⁻² year⁻¹; Hanrahan et al. 2018) to all unconstructed reaches of within the watershed. We performed this analysis under the theoretical conditions of ambient C floodwaters after 24 h of inundation.

Statistical analyses

To meet the assumptions of parametric statistics, we tested all data for normality with the Shapiro–Wilk test ($P > 0.05$). We determined significant DN using linear regression of N₂ or N₂O concentration versus incubation time ($p < 0.1$) following methods of Hanrahan et al. (2018). Each core within the same site and amendment were treated as a field replicate within a given inundation time ($n = 3$) if DN was significant by linear regression. We compared DN rates and floodplain characteristics using a three-way analysis of variance (ANOVA, $p < 0.05$), including [Inundation time × Site × Amend] as an interaction term to determine if the C amendment influenced denitrification at each experimental site over the different inundation times. We conducted all statistics in R (3.4.2).

Results

There were significant differences in floodplain soil characteristics between sites. Soil N (Fig. 2a) and C content (g kg dry soil⁻¹) (Fig. 2b) were significantly lower in the NEW floodplain compared to EST floodplains (t-test, $p < 0.001$ for both;), resulting in a 40% higher C:N ratio for soils at NEW (t-test, $p < 0.001$; Fig. 2c). Soil N content was positively correlated with soil organic matter (Pearson's r , $r = 0.85$, $P < 0.001$; Fig. 2d) as well as with soil C (Pearson's r , $r = 0.95$, $p < 0.001$; Fig. 2e). The correlations both grouped by site, whereby EST soils had higher organic matter (t-test, $p < 0.01$) compared to NEW. Soil C:N ratio was negatively correlated with organic matter (Pearson's r , $r = -0.78$, $p = 0.003$; Fig. 2f).

We found a linear increase in N₂O concentrations over incubation time (Fig. 3), indicating measurable *incomplete* denitrification (IDN), in 11 of 12 cores during the 0H inundation ($p < 0.1$, $r^2 = 0.44–0.79$), 3 of 12 cores during the 24H inundation ($p < 0.02$, $r^2 = 0.60–0.68$), and 2 of 12 cores during the 48H inundation ($p < 0.002$, $r^2 = 0.40–0.73$). Hourly rates of IDN ranged from 0.26 to 0.95 μg N₂O-N h⁻¹. Similarly, we found a linear increase in N₂ concentrations over the 8 h incubation time (Fig. 3), indicating measurable *complete* denitrification (CDN), in 10 of 12 cores during the 24H inundation ($p < 0.06$,

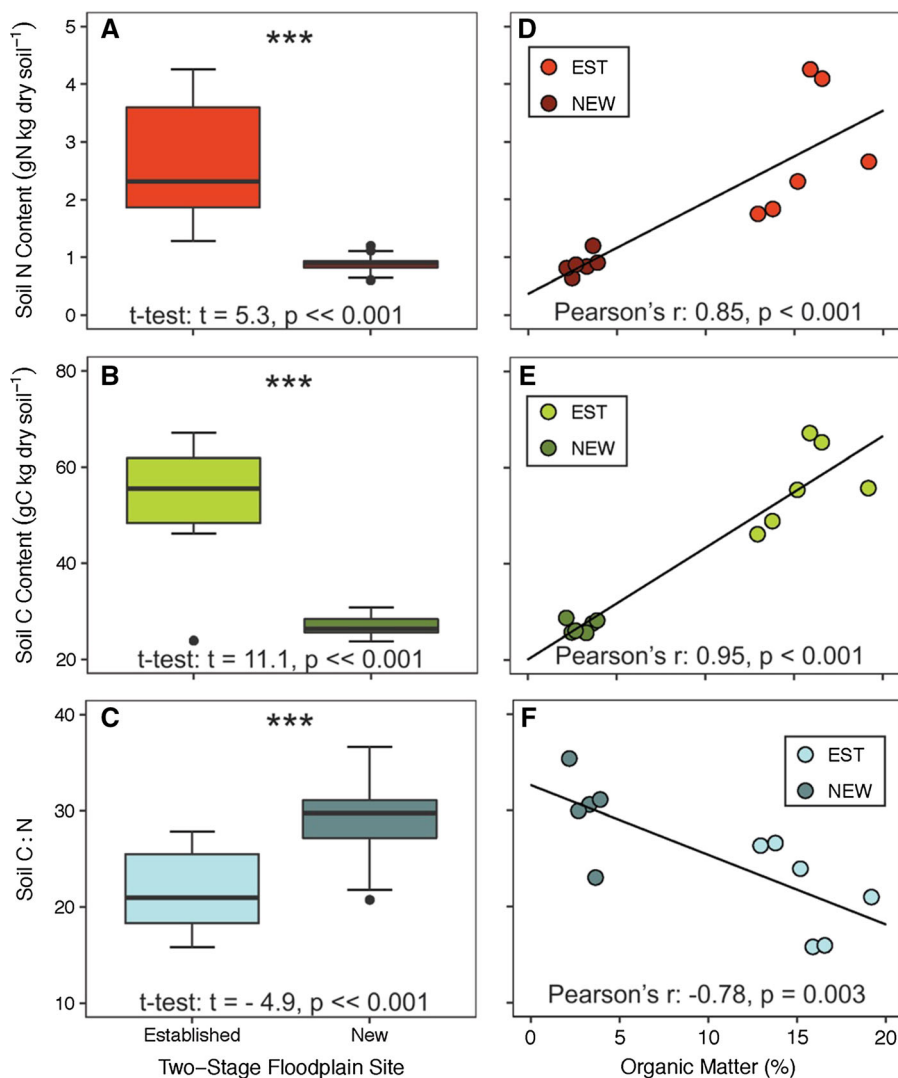


Fig. 2 Boxplots of floodplain soil characteristics, including **a** N content, **b** C content, and **c** C:N ratio by site. Means were compared by a two-sample t-test and coefficients are shown within each plot. Scatterplots of soil **d** N content, **e** C content,

and **f** C:N ratio versus soil organic matter (%) are evaluated by Pearson's correlation coefficient and the results are shown within each plot. Colors of points indicate site. (Color figure online)

$r^2 = 0.38$ – 0.90) and 7 of 12 cores during the 48H inundation ($p < 0.09$, $r^2 = 0.25$ – 0.71). None of the cores showed a significant N_2 increase during the 0HR inundation. Hourly rates of CDN ranged from 12.8 to 98.0 $\mu\text{g } N_2\text{-N } h^{-1}$. Considering both metrics of denitrification, only 4 of 36 cores showed both measurable CDN and ICN.

Using the rates calculated from each core, we can examine the effect of floodplain age, inundation time, and C amendments (+C) using denitrification expressed in three ways: $\mu\text{g } N \text{ m}^{-2} h^{-1}$, $\mu\text{g } N \text{ [g}$

$AFDM]^{-1} h^{-1}$, and $\mu\text{g } N \text{ [g DM]}^{-1} h^{-1}$. We visualized data among all factors (site, inundation time, and C amendment) to understand primary drivers of denitrification rates in these constructed sites (Fig. 4, left panels). First, DN_{DM} ranged from 0.0013 to 0.7357 $\mu\text{g } N \text{ [g DM]}^{-1} h^{-1}$ from all cores throughout all inundation times in each floodplain site. Expressed per unit organic matter, DN_{AFDM} ranged from 0.03 to 18.5 $\mu\text{g } N \text{ [g AFDM]}^{-1} h^{-1}$ in all cores, while areal DN ranged from 81.4 to 3,00,934.8 $\mu\text{g } N \text{ m}^{-2} h^{-1}$. Generally, DN_{DM} was $\sim 60\%$ lower in NEW cores

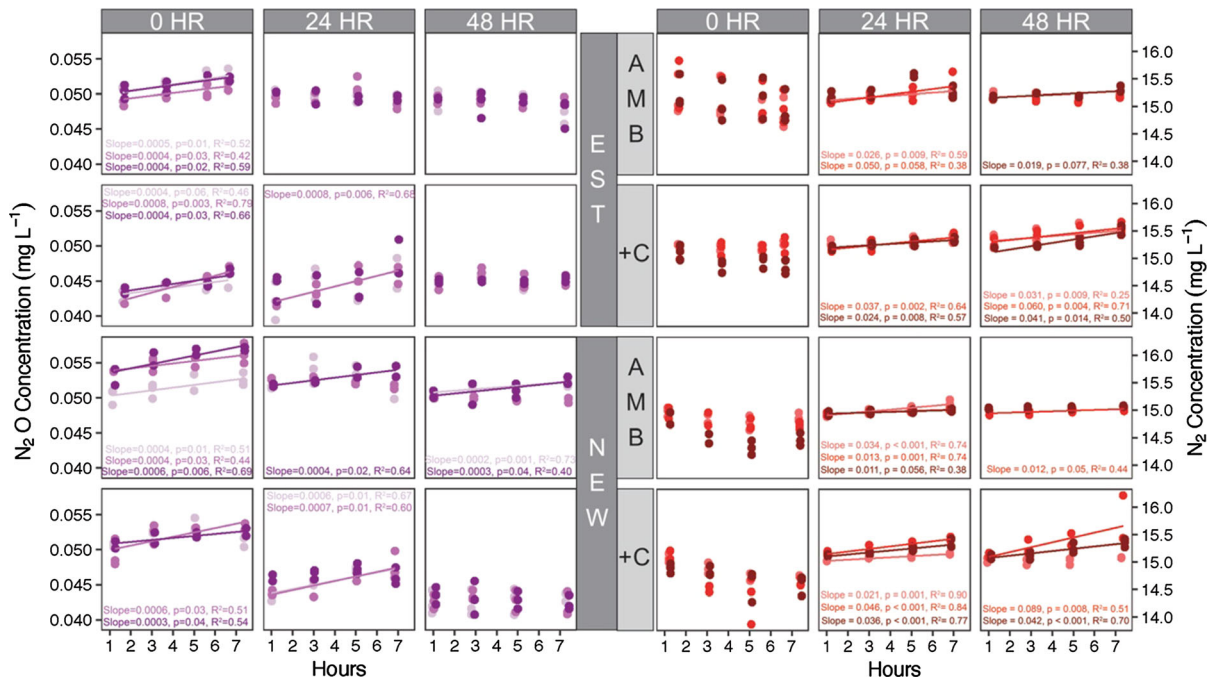


Fig. 3 N₂O (left side of figure) and N₂ (right side of figure) concentrations (in mg L⁻¹) versus incubation time in hours. Plots are faceted vertically by trial and horizontally by site and amendment, respectively. Data for all three field cores shown

than in EST (3-way ANOVA; Site: $F_{1,18} = 33.9$, $p < 0.0001$), but this variation differed with inundation time (3-way ANOVA; Inundation time x Site: $F_{2,18} = 9.2$, $p = 0.002$). However, when we analyzed floodplain site in the context of the other two factors, floodplain site was not a significant driver of areal denitrification or DN_{AFDM} (Fig. 4, left panels).

Given that floodplain site was not a major driver of denitrification in our study, we pared our analyses to include only inundation time and C amendment for each expression of denitrification (Fig. 4, right panels). A two-way ANOVA indicated that both inundation time and carbon amendment were significant drivers of denitrification (2-way ANOVA; inundation time: $F_{2,24} = 22.5$, $p < 0.0001$; amend: $F_{1,24} = 12.4$, $p < 0.002$). However, we found a significant interaction between inundation time and C amendment for all expressions of denitrification (2-way ANOVA; Inundation time x amend: $F_{2,24} = 9.14$, $p < 0.001$). Our results show that under both AMB and + C conditions, total denitrification significantly increases from 0 to 24 h of inundation time. However, total denitrification remains constant or decreases under ambient

(depicted by shade of point color), but only significant linear regressions ($p < 0.1$) are presented as lines on the plot. Coefficients for each significant linear regression are given within the facet of the relevant plot

conditions between 24 and 48 h of inundation. Conversely under the + C amendment, total denitrification increases between 24 and 48 h of inundation. Therefore, our data shows that both inundation time and C availability are significant drivers of total denitrification. Specifically, total denitrification increases with inundation time in until approximately 24 h of floodplain inundation, after which an additional source of C increases total denitrification after 48 h of inundation time. Given our novel analytical approach, supported by the MIMS instrumentation, we were also able to calculate the often-used N₂O yield (as $(N_2O/(N_2O + N_2)) * 100$) (Ciarlo et al. 2008; Beaulieu et al. 2011). In instances when no significant rate of production was detected for either gas, we assumed a rate of 0. We found that inundation time plays a significant role in the end-product of denitrification (Fig. 3), so we calculated a mean N₂O yield for each inundation time (0, 24, 48HR) by taking the average of all cores within a given site and C amendment ($n = 4$ per inundation time treatment). We found that N₂O yield dropped dramatically after

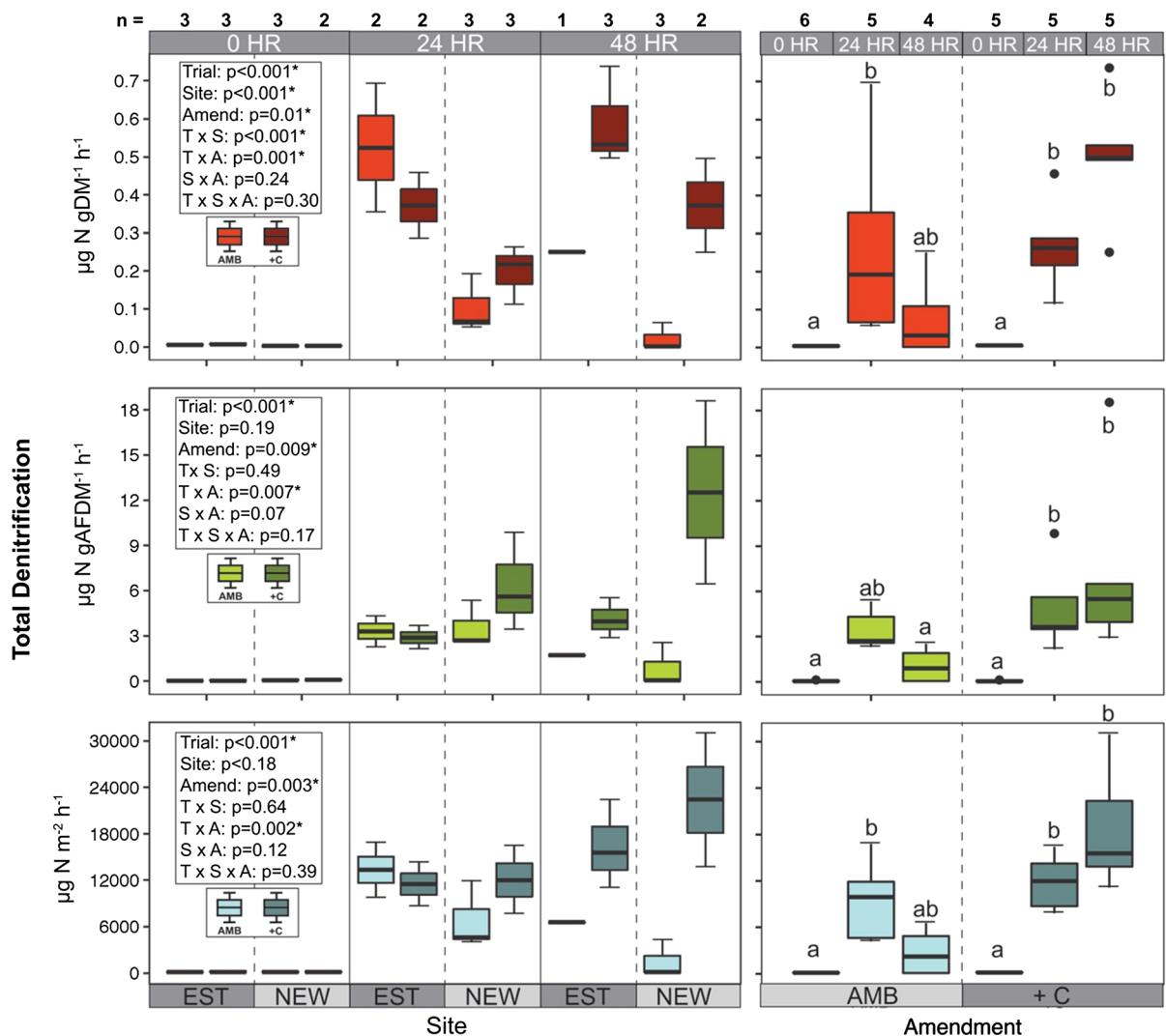


Fig. 4 Boxplots of denitrification rates expressed as $\mu\text{g N gDM}^{-1} \text{h}^{-1}$, $\mu\text{g N gAFDM}^{-1} \text{h}^{-1}$, and $\mu\text{g N m}^{-2} \text{h}^{-1}$. Plots on the left-side of figure are faceted by inundation time, amendment, and site. Box colors indicate the amendment and results of a 3-way ANOVA are shown within each plot. Given

the lack of significant difference between site, plots on right side of panel are faceted by inundation time and amendment. Lower case letters indicate significant differences (Tukey's HSD, $P < 0.05$)

initial inundation, with mean N_2O yields of 100% for 0HR, 0.78% for 24HR and 1.1% for 48HR (Fig. 7).

Finally, when we scaled up the areal denitrification rates for actual floodplain area of Shatto Ditch during two stages of restoration (Fig. 5), we found that the combination of constructed and “naturalized” floodplains could remove a significant amount of bioavailable N within the watershed. Upon the initial 600 m construction of floodplain (2007 period),

denitrification could potentially remove 0.6 kg N d^{-1} after 24 h of inundation and assuming an 8 h residence time. Upon restoration of all available stream length in the Shatto Ditch after 2017, denitrification could remove 4.9 kg N d^{-1} after 24 h of inundation. Therefore, constructed floodplains throughout Shatto Ditch in 2017 could potentially reduce N loads in stream water at a rate 8 times greater than in 2007.

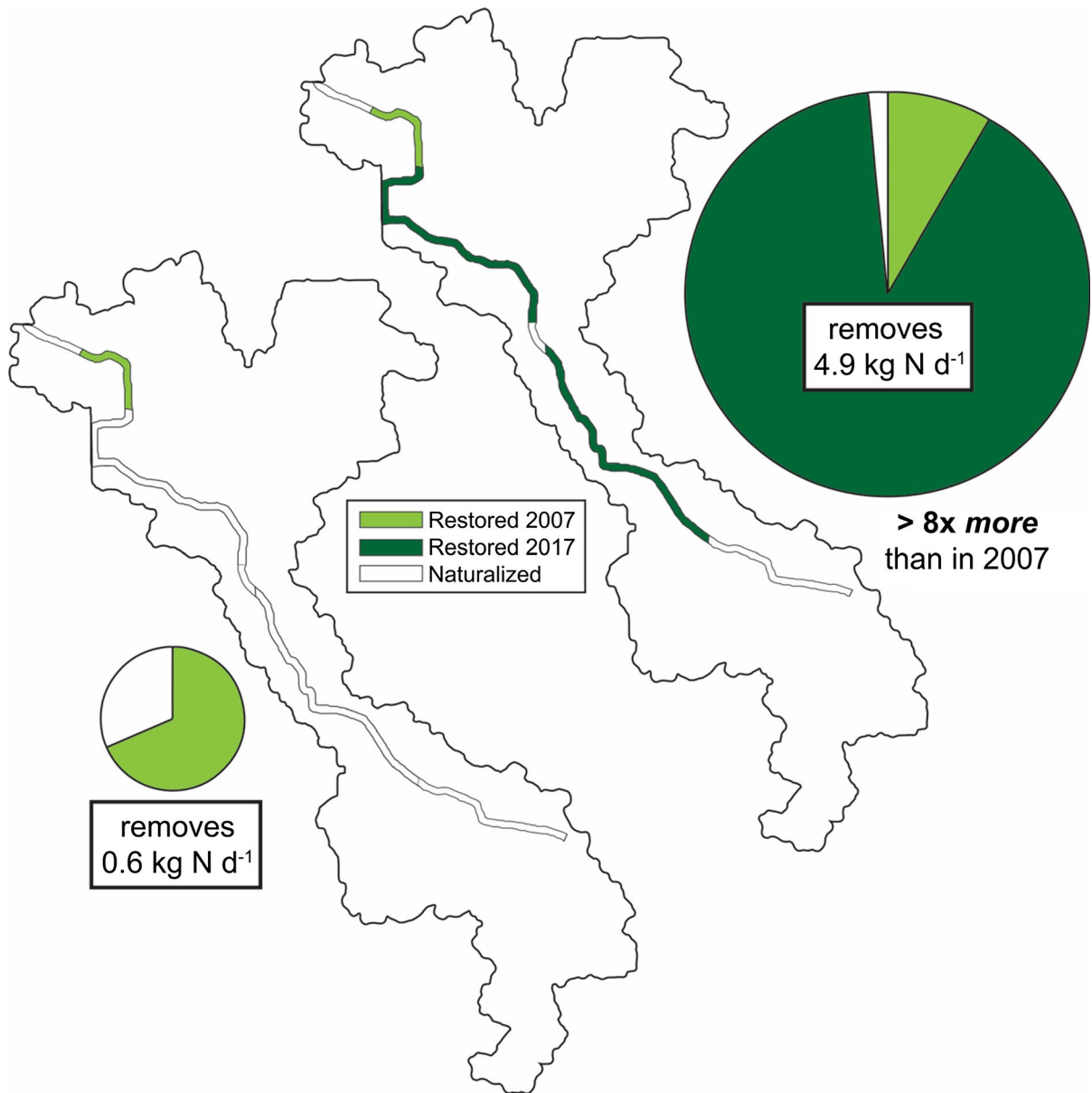


Fig. 5 Potential N removal via denitrification in the Shatto Ditch watershed during two stages of floodplain restoration: 2007 and 2017. Areas that have not been restored are considered

“naturalized” and a constant denitrification rate of $726 \mu\text{g N m}^{-2} \text{ year}^{-1}$ is applied. Inundation time is assumed to be 24 h

Discussion

Our study employed a novel in-situ, intact static core design to identify factors that control denitrification end-products in constructed floodplains of different ages. Results from this study underline the importance of floodplain restoration as mechanism to increase residence time of floodwaters on bioreactive surfaces,

allowing for increased removal of N via denitrification. We hypothesized that three factors would influence floodplain denitrification rates and subsequent N_2O yield: (1) floodplain age, (2) C limitation, and (3) inundation time. Briefly, we found that age did not influence denitrification, and rates did increase with duration of inundation, until C limitation became a driver after 24 h. Additionally, N_2O yields from

floodplains were higher than assumed previously (IPCC 2001), and while floodplain restoration can increase N retention in waterway, the impact of added floodplains on N₂O emissions should be considered.

Streamwater nitrate outweighs the impact of soil C and N heterogeneity on denitrification

We found that constructed floodplain soils were heterogeneous in composition and available soil C and N varied predictably with floodplain age. Available soil C and N increased with percent organic matter and were significantly higher in older floodplains (Fig. 2), which we hypothesized based on similar findings within the same watershed (Hanrahan et al. 2018) and other similar studies (McMillan and Noe 2017). Contrary to our hypothesis, we did not observe higher denitrification in the oldest floodplains. Previous research found that floodplain age increased channel stability (McMillan et al. 2014) and soil organic matter (Weier et al. 1993; McMillan and Noe 2017). Yet in this system, even newly constructed floodplains had the potential to remove N due to adequate soil C and NO₃-N delivery from adjacent stream water, which aligns with previous studies examining drivers of denitrification in floodplains (Groffman and Crawford 2003; Orr et al. 2007; Gift et al. 2010; Mahl et al. 2015). However, we must also address the potential impact of in-situ vegetation on FP site differences. While floodplain vegetation was dense on EST benches and could therefore not feasibly be excluded from our in situ cores, vegetation was sparse on NEW benches. The potential exists that oxygen produced by vegetation in EST cores may have influenced the ability of underlying soils to reach anoxia, thereby reducing denitrification in a FP site that we hypothesized would support greater denitrification.

To place our results in the context of other denitrification rates measured on constructed floodplains, we plotted areal DN (in $\mu\text{g N m}^{-2} \text{h}^{-1}$) versus water column NO₃⁻-N (in mg L^{-1} ; Fig. 6), using data from previously published studies in Shatto Ditch (Roley et al. 2012a, b; Mahl et al. 2015; Hanrahan et al. 2018). While all measurements were made in this same system, we note that both Roley et al. (2012a, b) and Mahl et al. (2015) estimated denitrification via the chloramphenicol-amended acetylene block technique on sediment slurries incubated in the laboratory, which

optimized redox conditions (Smith and Tiedje 1979; Royer et al. 2004; Arango et al. 2007). Hanrahan et al. 2018 also used slurries, but used the MIMS for analyses of dissolved N₂ only, implementing a sacrificial assay method, which places their results somewhere between potential and actual denitrification. We note that while these studies are comparable, slurries have lower water to sediment ratios than our cores, which assume that the entirety of enclosed floodplain soils may contribute to denitrification. Therefore, estimates of denitrification based on measurements using sediment slurries conducted under redox-optimized conditions may overestimate the in-situ rates presented in our study.

While our study period sits at the upper threshold of the baseflow NO₃⁻-N concentration range of the Shatto Ditch Watershed, denitrification measured with our in-situ static core method after 24 and 48 h of inundation indicate that denitrification within these floodplains soils are similar to those in other two-stage ditches, regardless of method and season (Roley et al. 2012a; Mahl et al. 2015; Hanrahan et al. 2018; Fig. 6). While floodplain denitrification responds linearly to instream nitrate concentrations under 1–2 $\text{mg NO}_3^- \text{N L}^{-1}$ (Hanrahan et al. 2018), we found that great variability exists in those floodplains with floodwaters exceeding that threshold. Under the conditions of our study, ambient floodwaters nitrate concentration (6.4–7.7 $\text{mg NO}_3^- \text{N L}^{-1}$) exceeded the point at which denitrification is saturated with respect to this particular reactant (Garcia-Ruiz et al. 1998; Hanrahan et al. 2018). Therefore we suggest that while constructed floodplains in this particular watershed are heterogeneous in form and function under saturated NO₃⁻-N conditions, these systems still possess the potential for significant NO₃⁻-N removal via denitrification.

Influence of C limitation on denitrification rates increases with inundation time

We documented denitrification in the floodplain soils in the Shatto Ditch within the first 8 h of inundation regardless of restoration age; however, the limitation of denitrification rate by C availability occurred between 24 and 48 h after inundation. Since restoration age was not a significant driver of denitrification rate (Fig. 3, left panel), we reduced our analysis to the factors of inundation time and C amendment (Fig. 3,

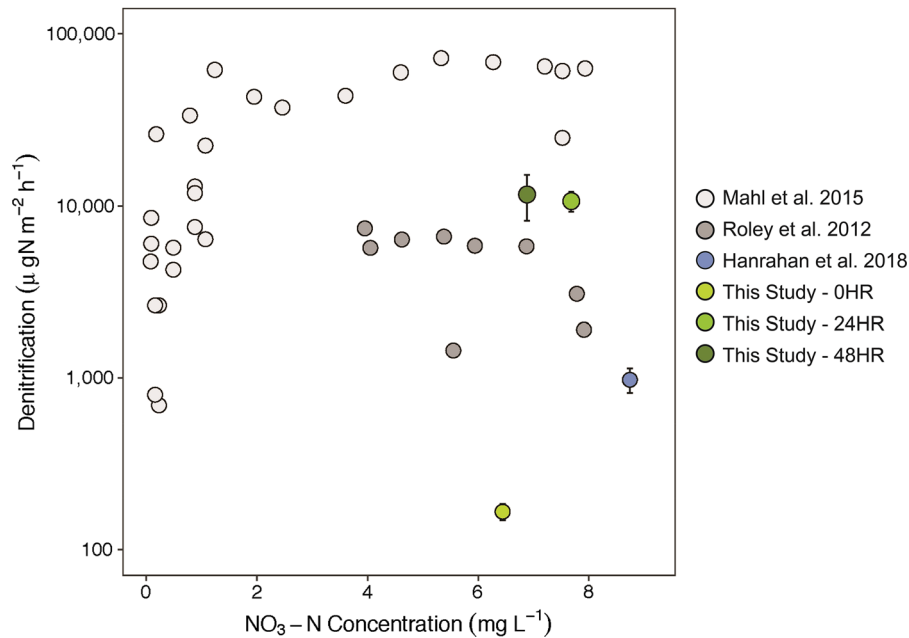


Fig. 6 Scatterplot of denitrification ($\mu\text{g N m}^{-2} \text{h}^{-1}$) versus nitrate concentration ($\text{mg NO}_3\text{-N L}^{-1}$) measured after 0 (light green), 24 (medium green), and 48 (dark green) hours of floodplain inundation in the context of previous studies conducted on two-stage floodplains (Roley et al. 2012a, b; Mahl et al. 2015; Hanrahan et al. 2018). Roley et al. and Mahl

et al. used the chloramphenicol-amended acetylene inhibition technique (Smith and Tiedje 1979; Royer et al. 2004) and Hanrahan et al. used sacrificial microcosm incubations with MIMS to estimate in-situ denitrification rates in laboratory assays

right panel). When expressed in $\mu\text{g N [g DM]}^{-1} \text{h}^{-1}$, denitrification increased between 0 and 24 h of inundation in both ambient and + C amended cores (Fig. 3, right panel). However, after 48 h of inundation under ambient conditions, total denitrification in floodplain soils appears to be limited by C availability; denitrification rate declines from 24 to 48 h in ambient cores, while rates increase under C addition. Previous studies in Shatto Ditch floodplains found that denitrification in constructed floodplain soils were not limited by C availability (Roley et al. 2012a, b; Mahl et al. 2015), however, they used the chloramphenicol-amended acetylene block technique (Smith and Tiedje 1979; Royer et al. 2004; Arango et al. 2007) on soil slurries, which did not directly test the role of inundation. Additionally, chloramphenicol-amended acetylene block technique of Roley et al. (2012a, b) and Mahl et al. (2015) inundates soils for only 4 h after extracting soils from the field. Similarly, the sacrificial slurry of Hanrahan et al. (2018) determines denitrification rate after soils are inundated for a total of only 8 h. While Roley et al. (2012a, b) found no C limitation of denitrification in the same floodplain

soils of our study using a method analogous to our 0HR inundation treatment, we suggest that this may be a result of limited inundation time. Therefore, we suggest that chloramphenicol-amended acetylene block or sacrificial slurry denitrification studies addressing C limitation in floodplain soils may find different results if soils are inundated prior to incubation.

Shifts from incomplete to complete denitrification occur with inundation time

We found that the contributions of N_2O to total denitrification in constructed floodplains were greatest immediately upon flooding, and that the end-product shifts from N_2O to N_2 over the course of 48 h of inundation. Within the first 8 h of flooding, regardless of whether they were recently constructed or well-established, floodplains exclusively produced N_2O (Fig. 3). After 24 h of continuous inundation, however, the majority of cores began producing the terminal end-product of denitrification (N_2). After 48 h, N_2O production nearly ceases and N_2 production

begins to taper as well. Previous studies have found that this transition from incomplete (terminus at N_2O) to complete (terminus at N_2) denitrification occurs as a result of NO_3-N limitation in soils; at higher soil NO_3-N concentrations, incomplete denitrification occurs as a result of the suppression of *nos* activity, which is the enzyme responsible for microbial conversion of N_2O to N_2 (Jalota et al. 2018; Weier et al. 1991; Firestone et al. 1979). Therefore, while our study replenished cores with a fresh supply of high NO_3-N water prior to each successive incubation, the transition from incomplete to complete denitrification may have occurred as underlying floodplain soils were depleted of NO_3-N within 0 to 24 h of inundation time.

While soil NO_3-N availability may primarily explain the transition from N_2O to N_2 production, inundation time and bioavailable C could influence denitrification end products. Previous studies have shown that with increasing anoxia, induced by water-filled pore space, the percentage of N_2 as the denitrification end-product increases (Rolston et al. 1978; Weier et al. 1993). Weier et al. (1993) simultaneously tested the combined effect of soil water content, C and NO_3-N availability on denitrification end-products, where N_2 was produced at the highest rate relative to N_2O under high C conditions. While we did not directly test the impact of inundation time on soil porewater anoxia, we suggest that a hierarchical framework exists by which chemical factors that influence microbial activity control the completion of denitrification as inundation time increases. That is, the successive depletion of NO_3-N and C from soils while soil anoxia increases may allow for idealized conditions for the microbial community to perform complete denitrification. Further exploration is required to identify the hierarchical control regarding NO_3-N , C availability, and inundation time on denitrification end-products, particularly for in-situ field-based experiments.

Floodplain N_2O yields differ strongly with inundation time

Even with incomplete denitrification, the concentration of N_2O produced is small relative to that of N_2 (Fig. 3) regardless of inundation time or C availability. Groffman et al. (2000) found that the N_2O yield may vary from 1:500 to 99:1 in riparian zones, indicating that this ratio is highly variable. Here we

place our N_2O yield estimates in the context of a previous meta-analysis (Beaulieu et al. 2011) for multiple ecosystem types including agricultural soils, marine, lake, stream, and other floodplain types (Fig. 7). We show that N_2O yields from our study differed strongly with inundation time, as cores produced N_2O yields at 100% immediately after inundation (0HR) and were significantly lower with longer inundation times (0.78% for 24HR and 1.1% for 48HR). Thus, 0HR cores may be comparable to high N_2O yields found in agricultural soils, but cores inundated for longer periods (24, 48HR) fall well within the lower range of for N_2O yields measured in other freshwater and marine systems. Additionally, the Intergovernmental Panel on Climate Change (IPCC) has used a N_2O yield of 0.5% for nitrification and denitrification in systems impacted by agricultural activity, termed “indirect emissions” (Nevison 2000; IPCC 2001), to calculate emission factors (EF) that inform global N_2O budgets. In a study by Tian et al. 2019 that informed the recent refinement of IPCC’s indirect N_2O EFs (IPCC 2019), the authors recognize the formative use of N_2O yields in developing EFs. We note that the mean N_2O yields generated from floodplain soils in our study exceed this static value of 0.5% (Fig. 7), particularly at shorter inundation times (0, 24 h). While we recognize the dynamic nature of estimating EFs and the iterative approach taken by the IPCC to do so effectively, we posit that this comparison reiterates how continued research aimed at constraining these estimates may have implications for global predictions and model parameterization.

Future research may use this field and MIMS-based methodology to isolate additional drivers of denitrification end products. In particular, evidence from numerous studies suggest that lower soil pH increases the likelihood of incomplete denitrification (Šimek and Cooper 2002) and understanding the role of pH management in the context of agricultural soils is critical (Adams and Adams 1983; Waring and Gilliam 1983). Previous studies in agricultural soils have cited several variables that impact yields from agricultural soils, including carbon availability, O_2 partial pressure, soil moisture content, pH and temperature (Nevison 2001). A comprehensive review by Saggar et al. (2013) concluded that the heterogeneity of soils and environmental conditions in these complex systems makes it difficult to accurately predict N_2O . For

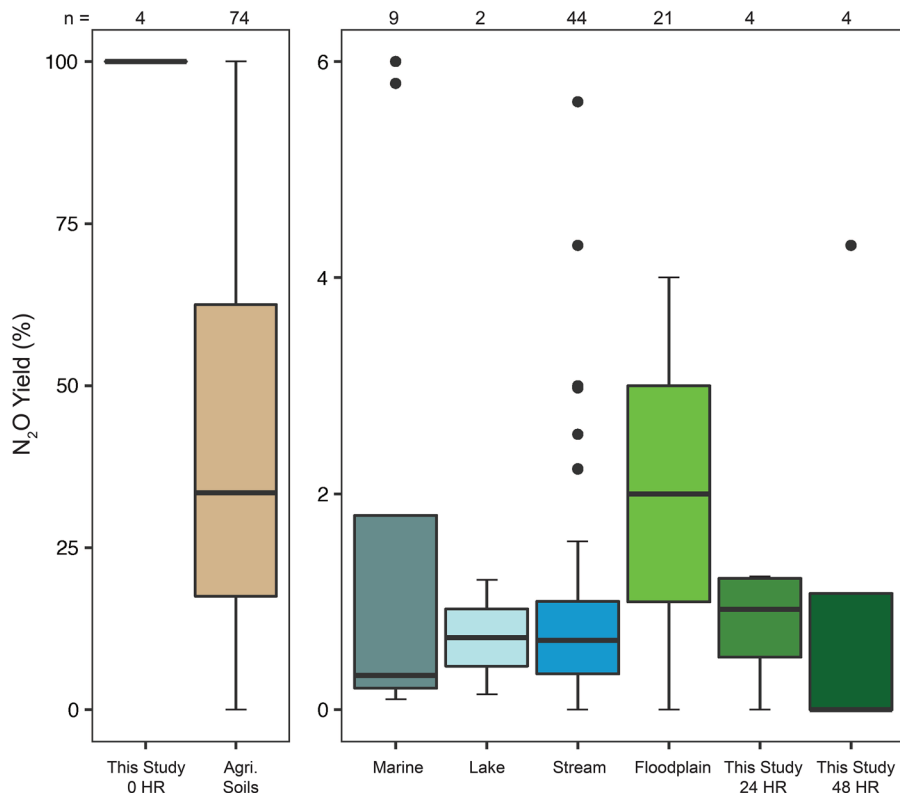


Fig. 7 Boxplots of nitrous oxide (N_2O) yield (percentage of denitrified N released as N_2O) measured in this study (separated by inundation time) in comparison with other ecosystems. The

example, Hénauld et al. (2012) describes considerable spatial and temporal variation for N_2O yield estimation found in the literature, emphasizing that the most variability is found at the smallest spatial scales ($< 1 \text{ m}^2$) and over the shortest time periods, which has direct implications for the study results described here. Moreover, this context emphasizes the ongoing challenges in understanding a complex transformation that occurs across a combination of heterogeneous soils/sediments and under very dynamic environmental conditions (Hénauld et al. 2012). In addition, while constructed floodplains may present a temporary source of N_2O to the atmosphere on very short timescales (i.e., $< 24 \text{ h}$), direct emissions from upland agricultural soils in the surrounding watershed far outweigh emissions from “indirect” aquatic sources that may occur as a result of agricultural runoff of fertilizer N. Many studies have suggested alternative ways to prevent agricultural land use from enhancing N_2O emissions, but Saggari et al. (2013) suggest that the difficulty of constraining N_2O yields “may explain

number of data points included in each boxplot is indicated at the top of the plot. Meta-analysis data modified from Beaulieu et al. (2011). Note the difference in scale between the two panels

why to date no clear picture has emerged as to the efficacy of soil management practices in reducing N_2O emissions”. However, Weier et al. (1993) suggested that decreasing application of N-based fertilizer may reduce $\text{NO}_3\text{-N}$ accumulation in soils and subsequently increase the conversion rate of N_2O to N_2 , while the best way to reduce N_2O emissions from agricultural watersheds may be to increase N use efficiency on farmlands (Hénauld et al. 2012).

Floodplain restoration jumpstarts N removal capacity of agricultural waterways

Floodplain restoration along the length of Shatto Ditch significantly accelerated N watershed scale N removal, regardless of the age of floodplain restoration. Constructed floodplains throughout the Shatto Ditch Watershed and currently remove $8 \times$ more N than if those same areas were allowed to naturalize (Fig. 5, right map), representing $\sim 4.9 \text{ kg N}$ removed per day. The floodplains constructed by

2017 (Fig. 5, shaded) flood regularly, with inundation times ranging from 50–150 days depending on the water year (Mahl et al. 2015), and they currently cover > 46% of the total stream length and represents the total area within the watershed available for restoration. In contrast, if restoration had stopped with 0.6 km in 2007, the short two-stage ditch and the remaining “naturalized” stream length would have removed only 0.6 kg N per day (Hanrahan et al. 2018; Fig. 5, left). Our study demonstrates that constructed floodplains increased permanent N removal from overlying water immediately upon inundation, and also triggered complete denitrification to N₂ after only 24 h of flooding. Given the role of inundation time in driving incomplete vs. complete denitrification, the role of storms will be a key driver of N₂O yields. Predicted increases in both the variability and intensity of precipitation are predicted for the Midwestern U.S., which are expected to increase water quality issues (Sinha et al. 2017), as such, floodplain restoration in agricultural headwaters could add resilience by increasing complete denitrification in order to mitigate downstream export of N.

Acknowledgements This research was supported by Illinois-Indiana Sea Grant College Program 074483-15949. MMD was supported in part by a University of Notre Dame Center for Environmental Science and Technology (CEST)/Bayer Predoctoral Fellowship. We thank numerous members of the Tank Lab for field and lab assistance, including Ursula Mahl and Abigail White. We are grateful to Annie Bowling of Dr. Todd Royer’s lab for sample analysis. We thank Dr. Sara McMillan for input on design; Dr. Todd Kana for valuable MIMS advisement; Jon Loftus and Suzyanne Guzicki of CEST for analytical instrument troubleshooting and Dr. Jason Taylor for an insightful review of an earlier version of this manuscript.

References

- Adams TM, Adams SN (1983) The effects of liming and soil pH on carbon and nitrogen contained in the soil biomass. *J Agric Sci* 101:553–558
- APHA (2012) Standard method for the examination of water and wastewater. American Public Health Association, Washington
- Arango CP, Tank JL, Schaller JL, Royer TV, Bernot MJ, David MB (2007) Benthic organic carbon influences denitrification in streams with high nitrate concentration. *Freshw Biol* 52:1210–1222. <https://doi.org/10.1111/j.1365-2427.2007.01758.x>
- Beaulieu JJ, Tank JL, Hamilton SK, Wollheim WM, Hall RO, Mulholland PJ et al (2011) Nitrous oxide emission from denitrification in stream and river networks. *PNAS* 108:214–219. <https://doi.org/10.1073/pnas.1011464108>
- Bernot MJ, Tank JL, Royer TV, David MB (2006) Nutrient uptake in streams draining agricultural catchments of the midwestern United States. *Freshw Biol* 51:499–509. <https://doi.org/10.1111/j.1365-2427.2006.01508.x>
- Bukaveckas PA (2007) Effects of channel restoration on water velocity, transient storage, and nutrient uptake in a channelized stream. *Environ Sci Technol* 41:1570–1576. <https://doi.org/10.1021/es061618x>
- Burgin AJ, Groffman PM (2012) Soil O₂ controls denitrification rates and N₂O yield in a riparian wetland. *J Geophys Res Biogeosci*. <https://doi.org/10.1029/2011JG001799>
- Burgin AJ, Groffman PM, Lewis DN (2010) Factors regulating denitrification in a riparian wetland. *Soil Sci Soc Am J* 74:1826–1833. <https://doi.org/10.2136/sssaj2009.0463>
- Carpenter SR, Caraco NF, Correll DL, Howarth RW, Sharpley AN, Smith VH (1998) Nonpoint pollution of surface waters with phosphorus and nitrogen. *Ecol Appl* 8:559–568. [https://doi.org/10.1890/1051-0761\(1998\)008\[0559:NPOSWW\]2.0.CO;2](https://doi.org/10.1890/1051-0761(1998)008[0559:NPOSWW]2.0.CO;2)
- Ciarlo E, Conti M, Bartoloni N et al (2008) Soil N₂O emissions and N₂O/(N₂O+N₂) ratio as affected by different fertilization practices and soil moisture. *Biol Fertil Soils* 44:991–995. <https://doi.org/10.1007/s00374-008-0302-6>
- Conrath U, Amoroso G, Kohle H, Sultemeyer DF (2004) Non-invasive online detection of nitric oxide from plants and some other organisms by mass spectrometry. *Plant J Cell Mol Biol* 38:1015–1022. <https://doi.org/10.1111/j.1365-313X.2004.02096.x>
- Firestone MK, Smith MS, Firestone RB, Tiedje JM (1979) The influence of nitrate, nitrite, and oxygen on the composition of the gaseous products of denitrification in soil. *Soil Sci Soc Am J* 43:1140–1144. <https://doi.org/10.2136/sssaj1979.03615995004300060016x>
- Galloway JN, Aber JD, Crisman JW, Seitzinger SP, Howarth RW, Cowling EB, Cosby BJ (2003) The nitrogen cascade. *Bioscience* 53:341–356. [https://doi.org/10.1641/0006-3568\(2003\)053\[0341:TNC\]2.0.CO](https://doi.org/10.1641/0006-3568(2003)053[0341:TNC]2.0.CO)
- Garcia-Ruiz R, Pattinson SN, Whitton BA (1998) Denitrification in river sediments: relationship between process rate and properties of water and sediment. *Freshw Biol* 39:467–476
- Genthner FJ, Marcovich DT, Lehrter JC (2013) Estimating rates of denitrification enzyme activity in wetland soils with direct simultaneous quantification of nitrogen and nitrous oxide by membrane inlet mass spectrometry. *J Microb Biochem Technol* 5:95–101. <https://doi.org/10.4172/1948-5948.1000108>
- Gift DM, Groffman PM, Kaushal SS, Mayer PM (2010) Denitrification potential, root biomass, and organic matter in degraded and constructed urban riparian zones. *Restor Ecol* 18:113–120
- Gihring TM, Canion A, Riggs A, Huettel M, Kostk JE (2010) Denitrification in shallow, sublittoral Gulf of Mexico permeable sediments. *Limnol Oceanogr* 55(1):43–54. <https://doi.org/10.4319/lo.2010.55.1.0043>
- Goodwin JM, Chrestensen CA, Moomaw EW (2018) Detection of nitric oxide by membrane inlet mass spectrometry. *Methods Mol Bio* 1747:35–47. https://doi.org/10.1007/978-1-4939-7695-9_4

- Griffiths NA, Tank JL, Royer TV, Roley SS, Rosi-Marshall EJ, Whiles MR et al (2013) Agricultural land use alters the seasonality and magnitude of stream metabolism. *Limnol Oceanogr* 58:1513–1529. <https://doi.org/10.4319/lo.2013.58.4.1513>
- Groffman PM, Holland EA, Myrold DD, Robertson GP, Zou X (1999) Denitrification. In: Robertson GP, Bledsoe CS, Coleman DC, Sollins P (eds) *Standard Soil Methods for Long-Term Ecological Research*. Oxford University Press, New York
- Groffman PM, Gold AJ, Addy K (2000) Nitrous oxide production in riparian zones and its importance to national emission inventories. *Chemosphere Global Change Sci* 2(3):291–299. [https://doi.org/10.1016/S1465-9972\(00\)00018-0](https://doi.org/10.1016/S1465-9972(00)00018-0)
- Groffman PM, Crawford MK (2003) Denitrification potential in urban riparian zones. *J Environ Qual* 32:1144–1149
- Hamme RC, Emerson SR (2004) The solubility of neon, nitrogen and argon in distilled water and seawater. *Deep Sea Res* 51:1517–1528. <https://doi.org/10.1016/j.dsr.2004.06.009>
- Hanrahan BR, Tank JL, Dee MM, Trentman MT, Berg EM, McMillan SK (2018) Constructed floodplains enhance denitrification compared to naturalized floodplains in agricultural streams. *Biogeochem* 141:419–437. <https://doi.org/10.1007/s10533-018-0431-4>
- Hénault C, Gossel A, Mary B, Roussel M, Léonard J (2012) Nitrous oxide emission by agricultural soils: a review of spatial and temporal variability for mitigation. *Pedosphere* 22(4):426–433. [https://doi.org/10.1016/S1002-0160\(12\)60029-0](https://doi.org/10.1016/S1002-0160(12)60029-0)
- IPCC (2001) *Climate change 2001: the scientific basis*. In: Houghton JT, Ding Y, Griggs DJ, Noguer M, van der Linden PJ, Dai X, Maskell K, Johnson CA (eds) *Contribution of working group I to the third assessment report of the intergovernmental panel on climate change*. Cambridge University Press, Cambridge
- IPCC (2007) *Climate change 2007. Contribution of working groups I, II and III to the fourth assessment report of the intergovernmental panel on climate change*. In: Pachauri RK, Reisinger A (eds) *Synthesis Report*. IPCC, Geneva, p 104
- IPCC (2019) *2019 Refinement to the 2006 IPCC Guidelines for National Greenhouse Gas Inventories, Volume 4: Agriculture, Forestry and Other Land Use*. Chapter 11: N₂O emissions from managed soils, and CO₂ emissions from lime and urea application. IPCC, Geneva
- Jalota SK, Vashisht BB, Sharma S, Kaur S (2018) Emission of greenhouse gases and their warming effect. In: Jalota SK, Vashisht BB, Sharma S, et al. (eds) *Understanding climate change impacts on crop productivity and water balance*. Academic Press, Cambridge, pp 1–53
- Kana TM, Darkangelo C, Hunt MD, Oldham JB, Bennett GE, Cornwell JC (1994) Membrane inlet mass spectrometer for rapid high-precision determination of N₂, O₂, and Ar in environmental water samples. *Anal Chem* 66:4166–4170. <https://doi.org/10.1021/ac00095a009>
- Kana TM, Sullivan MB, Cornwell JC, Groxzkowski KM (1998) Denitrification in estuarine sediments determined by membrane inlet mass spectrometry. *Limnol Oceanogr* 43:334–339. <https://doi.org/10.4319/lo.1998.43.2.0334>
- Kaushal SS, Groffman PM, Mayer PM, Striz E, Gold AJ (2008) Effects of stream restoration on denitrification in an urbanizing watershed. *Ecol Appl* 18:789–804
- Klein CD, Novoa RSA, Ogle S, Smith KA, Rocette P, Wirth TC (2006) N₂O emissions from managed soils, and CO₂ emissions from lime and urea application. In: 2006 IPCC guidelines for national greenhouse gas inventories. Intergovernmental Panel on Climate Change. Available at https://www.ipcc-nggip.iges.or.jp/public/2006gl/pdf/4_Volume4/V4_11_Ch11_N2O&CO2.pdf
- Knowles R (1982) Denitrification. *Microbiol Rev* 46:43–70
- Landwehr K, Rhoads BL (2003) Depositional response of a headwater stream to channelization, East Central Illinois, USA. *River Res Appl* 19:77–100. <https://doi.org/10.1002/rra.699>
- Letey J, Valoras N, Hadas A, Focht DD (1980) Effect of air-filled porosity, nitrate concentration, and time on the ratio of N₂O/N₂ evolution during denitrification. *J Env Qual* 9:227–231. <https://doi.org/10.2134/jeq1980.00472425000900020013x>
- Mahl UH, Tank JL, Roley SS, Davis RT (2015) Two-stage ditch floodplains enhance N-removal capacity and reduce turbidity and dissolved P in agricultural streams. *J Am Water Resour Assoc* 51:923–940. <https://doi.org/10.1111/1752-1688.12340>
- McMillan SK, Tuttle AK, Jennings GD, Gardner A (2014) Influence of restoration age and riparian vegetation on reach-scale nutrient retention in constructed urban streams. *J Am Water Resour Assoc* 50:626–638. <https://doi.org/10.1111/jawr.12205>
- McMillan SK, Noe G (2017) Increasing floodplain connectivity through urban stream restoration increases nutrient and sediment retention. *Ecol Eng* 108:284–295. <https://doi.org/10.1016/j.ecoleng.2017.08.006>
- Nevison C (2000) Review of the IPCC methodology for estimating nitrous oxide emissions associated with agricultural leaching and runoff. *Chemosphere Global Change Sci* 2(3–4):493–500. [https://doi.org/10.1016/S1465-9972\(00\)00013-1](https://doi.org/10.1016/S1465-9972(00)00013-1)
- Nevison C (2001) Indirect N₂O Emissions from Agriculture. In: *Good practice guidance and uncertainty management in national greenhouse gas inventories*. Intergovernmental Panel on Climate Change. Available at <https://www.ipcc-nggip.iges.or.jp/public/gp/english/>
- Orr CH, Stanley EH, Wilson KA, Finlay JC (2007) Effects of restoration and reflooding on soil denitrification in a leveed midwestern floodplain. *Ecol Appl* 17:2365–2376. <https://doi.org/10.1890/06-2113.1>
- Phillips RL, McMillan AMS, Palmada T, Dando J, Giltrap D (2015) Temperature effects on N₂O and N₂ denitrification end-products for a New Zealand pasture soil. *N Z J Agric Res* 58:89–95. <https://doi.org/10.1080/00288233.2014.969380>
- Powell GE, Ward AD, Mecklenburg DE, Jayakaran AD (2007) Two-stage channel systems: part 1, a practical approach for sizing agricultural ditches. *J Soil Water Conserv* 62:277–286
- Powell KL, Bouchard V (2010) Is denitrification enhanced by the development of natural fluvial morphology in agricultural headwater ditches? *J N Am Benthol Soc* 29:761–773. <https://doi.org/10.1899/09-028.1>

- Randall GW, Huggins DR, Russelle MP, Fuchs DJ, Nelson WW, Anderson JL (1997) Nitrate losses through subsurface tile drainage in conservation reserve program, alfalfa, and row crop systems. *J Env Qual* 26:1240–1247. <https://doi.org/10.2134/jeq1997.00472425002600050007x>
- Roley SS, Tank JL, Stephen ML, Johnson LT, Beaulieu JJ, Witter JD (2012a) Floodplain restoration enhances denitrification and reach-scale nitrogen removal in an agricultural stream. *Ecol Appl* 22:281–297. <https://doi.org/10.1890/11-0381.1>
- Roley SS, Tank JL, Williams MA (2012b) Hydrologic connectivity increases denitrification in the hyporheic zone and constructed floodplains of an agricultural stream. *Geophys Res* 117:G00NO4. <https://doi.org/10.1029/2012JG001950>
- Roley SS, Tank JL, Griffiths NA, Hall RO, Davis RT (2014) The influence of floodplain restoration on whole-stream metabolism in an agricultural stream: insights from a 5-year continuous data set. *Freshw Sci* 33:1043–1059. <https://doi.org/10.1086/677767>
- Rolston DE, Hoffman DL, Toy DW (1978) Field measurement of denitrification: I. flux of N_2 and N_2O . *Soil Sci Soc Am Journal* 42:863–869. <https://doi.org/10.2136/sssaj1978.03615995004200060004x>
- Royer TV, Tank JL, David MB (2004) Transport and fate of nitrate in headwater agricultural streams in Illinois. *J Environ Qual* 33:1296–1304. <https://doi.org/10.2134/jeq2004.1296>
- Ryden JC, Lund LJ, Letey J, Focht DD (1979) Direct measurement of denitrification loss from soils: II. Development and application of field methods. *Soil Sci Soc Am J* 43:110–118. <https://doi.org/10.2136/sssaj1979.03615995004300010020x>
- Saggar S, Jha N, Deslippe J, Bolan NS, Luo J, Giltrap DL, Kim D-G, Zaman M, Tillman RW (2013) Denitrification and $N_2O:N_2$ production in temperate grasslands: processes, measurements, modelling and mitigating negative impacts. *Sci of The Tot Env* 465:173–195. <https://doi.org/10.1016/j.scitotenv.2012.11.050>
- Schlüter M, Gentz T (2008) Application of membrane inlet mass spectrometry for online and in situ analysis of methane in aquatic environments. *J Am Soc for Mass Spectrom* 19:1395–1402. <https://doi.org/10.1016/j.jasms.2008.07.021>
- Sheibley RW, Ahearn DS, Dahlgren RA (2006) Nitrate loss from a constructed floodplain in the Lower Cosumnes River, California. *Hydrobiologia* 571:261–272. <https://doi.org/10.1007/s10750-006-0249-2>
- Šimek M, Cooper JE (2002) The influence of soil pH on denitrification: progress towards the understanding of this interaction over the last 50 years. *Eur J Soil Sci* 53:345–354. <https://doi.org/10.1046/j.1365-2389.2002.00461.x>
- Sinha E, Michalak AM, Balaji V (2017) Eutrophication will increase during the 21st century as a result of precipitation changes. *Science* 357:405–408
- Smith KA, Ball T, Conen F, Dobbie KE, Massheder J, Rey A (2003) Exchange of greenhouse gases between soil and atmosphere: interactions of soil physical factors and biological processes. *European J Soil Sci* 54:779–791. <https://doi.org/10.1046/j.1351-0754.2003.0567.x>
- Smith MS, Tiedje JM (1979) The effect of roots on soil denitrification. *Soil Sci Soc Am J* 43:951–955. <https://doi.org/10.2136/sssaj1979.03615995004300050027x>
- Tian L, Cai Y, Akiyama H (2019) A review of indirect N_2O emission factors from agricultural nitrogen leaching and runoff to update of the default IPCC values. *Environ Pollut* 245:300–306. <https://doi.org/10.1016/j.envpol.2018.11.016>
- Vinther FP (1984) Total denitrification and the ratio between N_2O and N_2 during the growth of spring barley. *Plant Soil* 76:227–232. <https://doi.org/10.1007/BF02205582>
- Vitousek PM, Aber JD, Howarth RW, Likens GE, Matson PA, Schindler DW et al (1997) Technical report: human alteration of the global nitrogen cycle: sources and consequences. *Ecol Appl* 7:737–750. <https://doi.org/10.2307/2269431>
- Waring SA, Gilliam JW (1983) The effect of acidity on nitrate reduction and denitrification in lower coastal plain soils. *Soil Sci Soc Am J* 47:246–251
- Weier KL, Doran JW, Power JF, Walters DT (1993) Denitrification and the dinitrogen/nitrous oxide ratio as affected by soil water, available carbon, and nitrate. *Soil Sci Soc Am J* 57:66–72. <https://doi.org/10.2136/sssaj1993.03615995005700010013x>
- Weier KL, Macrae IC, Myers RJK (1991) Seasonal variation in denitrification in a clay soil under a cultivated crop and a permanent pasture. *Soil Biol Biochem* 23:629–635. [https://doi.org/10.1016/0038-0717\(91\)90075-U](https://doi.org/10.1016/0038-0717(91)90075-U)

Publisher's Note Springer Nature remains neutral with regard to jurisdictional claims in published maps and institutional affiliations.